

Ultrasonic-attenuation investigation of the mixed state in three vanadium samples of varying purity*

J. A. Waynert,[†] H. Salvo, Jr., S. Schneider, and M. Levy

Department of Physics, University of Wisconsin—Milwaukee, Milwaukee, Wisconsin 53201

(Received 8 April 1976)

Ultrasonic-attenuation measurements were performed in three single-crystal vanadium samples, with resistivity ratios of 7.8, 245, and 450 as a function of magnetic field and temperature. Measurements obtained as a function of applied magnetic field were compared to the theoretical predictions of Houghton and Maki (HM) for the region near H_{c2} . Because of the varying purity of the samples, the HM predictions for the dependence of the normalized attenuation on mean free path were also tested. In all cases, the experimental results were in good qualitative agreement with the HM predictions. Ultrasonic-attenuation measurements as a function of temperature compared well to the BCS theory and yielded critical temperatures of 4.69, 5.26, and 5.27°K with corresponding zero temperature energy gaps of $2\Delta(0)/kT_c = 3.6, 3.6, \text{ and } 3.5$ in order of increasing sample purity.

I. INTRODUCTION

Acoustic-absorption measurements were performed as a function of temperature and magnetic field in three different-purity vanadium samples with resistivity ratios (Γ) of 7.8, 245, and 450, to be referred as samples I, II, and III, respectively. The data obtained in the normal state were related to Pippard's¹ free-electron theory for ultrasonic attenuation to provide information about the electron mean-free paths and to test the quality of the transducer bonds. Measurements as a function of temperature were compared to the BCS predictions² to yield the critical temperatures and the temperature-dependent energy gaps. However, the greatest emphasis has been placed on the data obtained in the mixed state near the upper critical field H_{c2} , where the magnetization is small and depends linearly⁴ on $H_{c2} - H \equiv \Delta H$ (H is the applied field). In this instance, detailed comparisons were made to the theory of Houghton and Maki³ (hereafter HM) which describes the normalized attenuation $(\alpha_n - \alpha_s)/\alpha_n \equiv \Delta\alpha/\alpha$ (n —normal, s —superconducting) in terms of a single, dimensionless parameter

$$\mu = (2\sqrt{\pi}/\hbar^2) (\Delta/k_c v_F)^2 k_c l,$$

where Δ is the spatially averaged order parameter, k_c is the reciprocal-lattice vector of the vortex lattice, v_F is the Fermi velocity, and l is the electronic mean-free path. This parameter μ can be expressed in terms of experimental observables with the result $\mu = f(t)\Delta H$, where $f(t)$ is a function of the reduced temperature t .

In this paper, the normalized attenuation as a function of H is directly compared to the normalized attenuation as a function of μ ; two independent methods of experimentally determining $f(t)$ are

presented, as well as supporting information obtained from the energy-gap and normal-state data. These data are presented for all three samples. The results appear to experimentally corroborate the HM theory.

II. THEORY

The starting point of the HM approach to ultrasonic attenuation in the mixed state is to write down the damping factor for this nonequilibrium process and solve for the imaginary (absorptive) part, which is just the attenuation in the superconducting state α_s . Thus, the rate of energy absorption is proportional to the square of the matrix element for the transition probability times essentially the product of the density of initial and final states, i.e., the product of the Green's functions. For this purpose, HM use the Green's function derived by Brandt, Pesch, and Tewordt.⁵

The transition probability depends on the orientation of the magnetic field relative to the direction of propagation. For transverse waves, the polarization is also important. For consistency in comparison of the data, transverse waves with phonon wave vector \vec{q} parallel to \vec{H} and ion motion \vec{u} perpendicular to \vec{H} were propagated in all three samples. The corresponding HM expression for the attenuation in this configuration is

$$\Delta\alpha/\alpha = 15\mu \left[\mu^2(1 - \mu^2) J_1 + \frac{1}{16}\pi - \frac{1}{3}\mu - \frac{1}{4}\mu\pi^2 + \mu^3 \right], \quad (1)$$

where

$$J_1 = \frac{\pi}{2} - \frac{2\mu}{(\mu^2 - 1)^{1/2}} \tan^{-1} \left(\frac{\mu - 1}{\mu + 1} \right)^{1/2}.$$

(The quantitative and qualitative behavior of this function has been discussed in Ref. 6.)

III. EXPERIMENT

A Matec ultrasonic attenuation system in the double echo mode was used to perform our pulse-echo measurements. In sample I, both longitudinal waves (135 MHz) and transverse waves (255 MHz, polarized $\langle 1\bar{1}0 \rangle$) were propagated in the $\langle 110 \rangle$ direction. In sample II, transverse waves with a frequency of 15 MHz in the $\langle 110 \rangle$ direction and polarized in the $\langle 1\bar{1}0 \rangle$ direction were propagated. In sample III, 45 MHz transverse waves in the $\langle 100 \rangle$ direction were used. In all cases, the applied magnetic field was parallel to the direction of propagation. (For greater detail on the experimental apparatus or procedures, see Ref. 6.) Table I lists the relevant sample parameters.

A typical field run involved sweeping the magnetic field from zero to a value approximately 20% greater than H_{c2} and sweeping back to zero. During this process the temperature was held constant. After each run, the sample was returned to the virgin state by heating it to about 30 °K for 8 min. Field runs were performed at constant temperatures ranging typically from 1.5 °K to the critical temperature T_c in 0.25° steps.

IV. ANALYSIS

A. Houghton-Maki parameter $\mu = f(t)\Delta H$

To facilitate the comparison of theory and experiment, the HM parameter $\mu = 2\sqrt{\pi}(\Delta/\hbar k_c v_F)^2 k_c l$ must first be expressed in terms of measurable parameters. The reciprocal-lattice vector is $k_c = (2\pi H_{c2}/\phi_0)^{1/2}$, where the flux quantum $\phi_0 = 2.07 \times 10^{-7}$ Gcm², and the square of the spatially-averaged order parameter can be related⁴ to the magnetization by

$$\Delta^2 \equiv \langle |\Delta|^2 \rangle = \frac{-4\pi^2 M}{m p_F} \left(H_{c2}(t) - \frac{t}{2} \frac{dH_{c2}}{dt} \right), \quad (2)$$

where

$$-4\pi M = (H_{c2} - H) / [\beta(2\kappa_2^2 - 1) + n]. \quad (3)$$

(This expression defines κ_2 and $\beta = 1.16$.) Here

$N(0) = m p_F / 2\pi^2$ is the density of states per spin at the Fermi surface, and n is the demagnetization factor. The resulting relationship is

$$\mu = - \frac{4l}{\hbar^2 v_F^2 N(0)} \left(\frac{\phi_0}{2H_{c2}} \right)^{1/2} \left(H_{c2}(t) - \frac{t}{2} \frac{dH_{c2}}{dt} \right) M \equiv f(t)\Delta H, \quad (4)$$

where

$$f(t) = \frac{l}{\hbar^2 v_F^2 N(0)} \left(\frac{\phi_0}{H_{c2}} \right)^{1/2} \times \left(H_{c2}(t) - \frac{t}{2} \frac{dH_{c2}}{dt} \right) \frac{1}{\beta(2\kappa_2^2 - 1) + n}. \quad (5)$$

Since the normalized attenuation $(\alpha_n - \alpha_s)/\alpha_n$ is described by μ , then at a constant temperature the attenuation is also described by $H_{c2} - H \equiv \Delta H$.

1. First experimental method of determining $f(t)$

The experimental procedure involved measuring the attenuation α_s as a function of the applied magnetic field H for fixed values of temperature. Figure 1 shows representative raw data graphs for samples I and II. These figures illustrate that H_{c2} and α_n may easily be read off the graphs. The behavior near H_{c1} (~200 G in sample I and ~900 G in sample II) will be discussed later in this article.

That portion of the graphs for H near H_{c2} , typically $0.2(H_{c2} - H_{c1})$ in samples II and III, but as much as $0.8(H_{c2} - H_{c1})$ in sample I, was then digitized, and the results were fed to a Univac 1110 computer. Two tables, one of the theoretical values of $\Delta\alpha/\alpha$ vs μ and one of the experimental values of $\Delta\alpha/\alpha$ vs ΔH , were compiled. For a given experimental value of the normalized attenuation, a value of μ and a value of ΔH were found from these two tables. The computer was then used to provide a linear least-squares fit of μ to ΔH , where the slope of this least-square fit at reduced temperature t is $f(t) = \mu/\Delta H$. The value of H_{c2} was appropriately adjusted to make the line intersect the origin. The shift in H_{c2} never amounted to more than a 2% change from the visually obtained value. Figure 2 shows the resulting linear relationship for samples I-III. In samples II and III, a proposed⁷⁻¹⁰ one-dimensional fluctuation effect dominates the electron-phonon

TABLE I. Relevant sample parameters.

Sample	$\Gamma(\rho/\rho_0)$	Length (cm)	Diameter (cm)	Cylinder		
				axis	ρ ($\mu\Omega$ cm)	ρ_0 ($\mu\Omega$ cm)
I	7.8	3.94	0.61	[110]	22	2.8
II	245	3.78	0.63	[110]	21	0.087
III	450	0.62	0.37	[100]	23	0.052

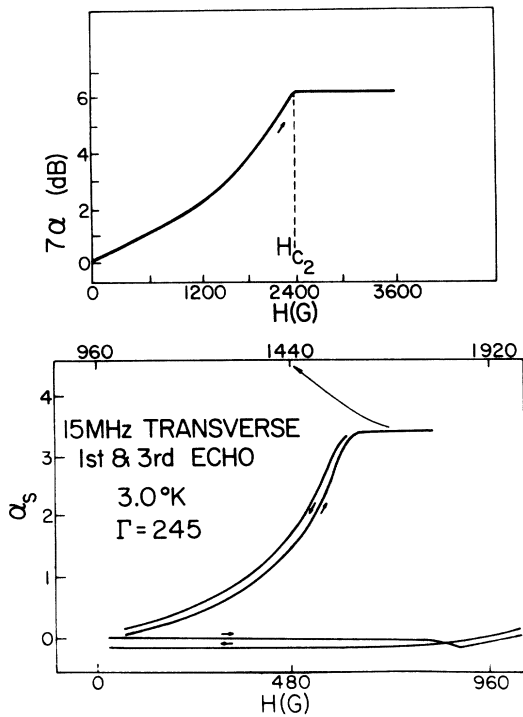


FIG. 1. Raw data of attenuation vs applied magnetic field for (a) sample I, 135 MHz, $T = 3.6^\circ\text{K}$, longitudinal wave and (b) sample II, 15 MHz, $T = 3.0^\circ\text{K}$, transverse waves.

interaction very near H_{c2} causing a rounding in the attenuation. This effect has not been included in the HM theory; therefore, data obtained for extremely small values of H , those in the convex part of the curve of α_s vs H , were intentionally discarded for this analysis in samples II and III. The effect appeared to be minimal in sample I.

Once the proportionality constant $f(t)$ between μ and ΔH was obtained, the theory [Eq. (1)] and the digitized experimental points were compared for that temperature. The results for several temperatures can be seen in Fig. 3.

2. Second experimental method of determining $f(t)$

An independent method of arriving at $f(t) = \mu/\Delta H$ was used in comparing the HM theory to the experimental results. The method required determining H_{c2} , κ_2 , and l as functions of temperature. These values could then be substituted into Eqs. (4) and (5) to arrive at a continuous functional relationship between μ and ΔH for all t .

(a) H_{c2} as a function of temperature. The values of H_{c2} for each temperature could easily be read off the raw data curves, but, for self-consistency, adjusted values were used. These values were determined by a linear least-squares fit of μ to

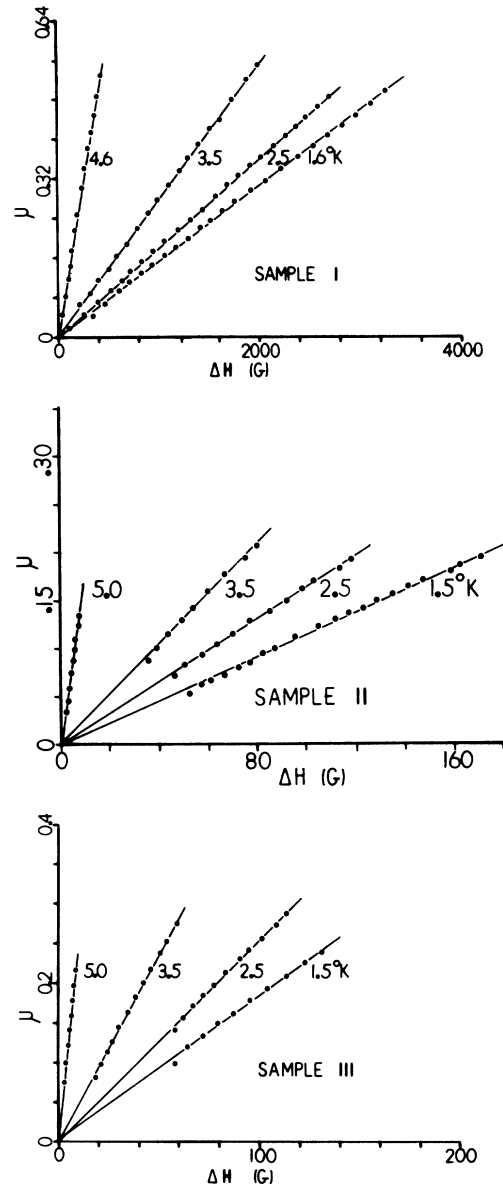


FIG. 2. Linear relationship between μ and ΔH for several temperatures in samples I-III. Slope of line, $\mu/\Delta H$, is the value of $f(t)$ at that temperature.

ΔH as described previously. The critical temperature could also be obtained from this data by extrapolating to H_{c2} equal zero, yielding $T_c = 4.81$, 5.26 , and 5.34 K for samples I-III, respectively. A modified equation for Abrikosov and Ginsburg's¹¹ $\kappa_1(t)$ incorporating a fitting parameter a , and a quadratic temperature dependence for $H_c(t)$ was used to empirically determine $H_{c2}(t) = H_{c2}(0)(1 - t^2)/(1 + at^2)$. $H_{c2}(0)$ and a for each sample can be found in Fig. 4 which also illustrates the comparison of the experimental points for H_{c2} and the

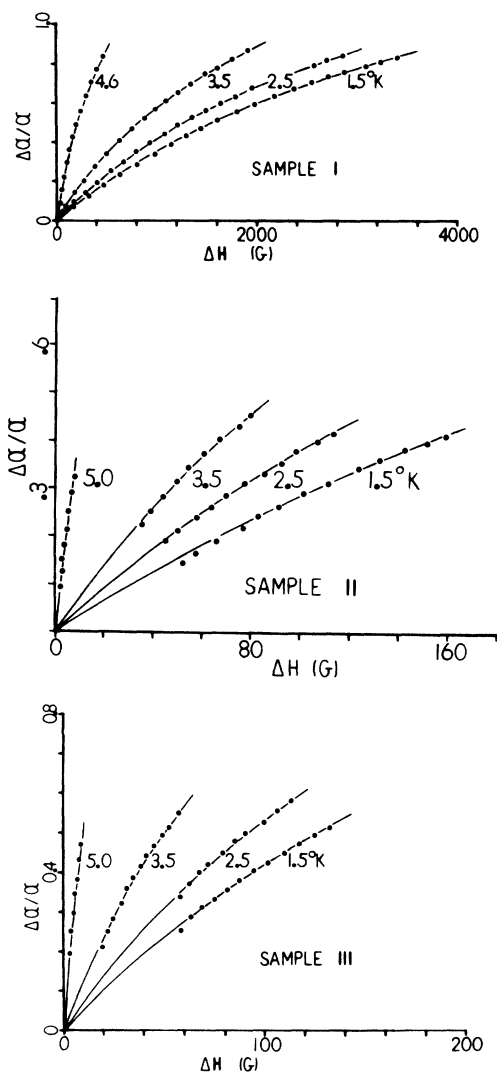


FIG. 3. HM theory vs experiment in samples I–III. HM theory [Eq. (1)], smooth curve, vs the digitized experimental points at several temperatures.

empirically determined values for all three samples. Therefore, part of Eq. (5) is reduced to:

$$\left(\frac{\phi_0}{2H_{c2}(t)}\right)^{1/2} \left(H_{c2}(t) - \frac{t}{2} \frac{dH_{c2}}{dt}\right) = \left(\frac{\phi_0 H_{c2}(0)}{2}\right)^{1/2} \frac{1 + 2at^2 - at^4}{(1-t^2)^{1/2} (1+at^2)^{3/2}} \quad (6)$$

The demagnetization factor n was estimated from sample dimensions and the theoretical results of Osborn.¹² The calculated values are $n = 0.036$, 0.043 , and 0.12 for samples I–III, respectively, for the applied field parallel to the cylindrical axis of each specimen.

(b) κ_2 as a function of temperature. κ_2 as a function of temperature and mean-free path was de-

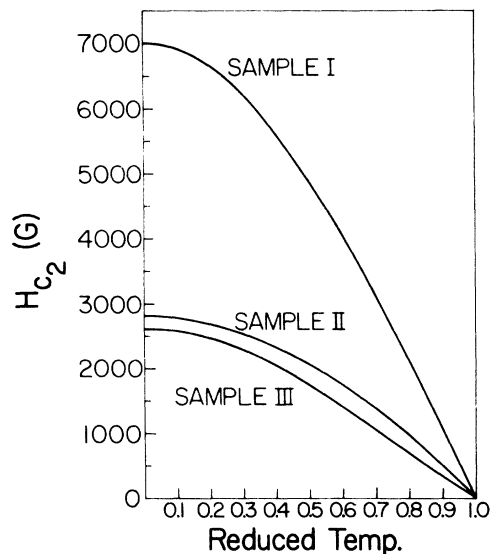


FIG. 4. H_{c2} as a function of the reduced temperature. Experimental data are compared to the empirically determined equation $H_{c2}(t) = H_{c2}(0) (1-t^2)/(1+at^2)$ where $H_{c2}(0) = 7000$, 2800 , and 2625 G and $a = 0.3$, 0.6 , and 0.55 for samples I–III, respectively.

termined in two different ways. One method was based on the experimental results of Auer and Ullmaier¹³ who showed that κ_2 was a linear function of the residual resistance at any fixed temperature. In order to make use of their finding, it was assumed that the inverse of the resistivity ratio was a direct measure of the residual resistance. With this information, a table listing κ_2 vs $1/\Gamma$ was established for various temperatures, using the magnetization data on vanadium obtained by Sekula and Kernohan¹⁴ for $\Gamma = 450$, and by Radebaugh and Keesom¹⁵ for $\Gamma = 140$. Thus $\kappa_2(t)$ values for samples II and III, with resistivity ratios of 245 and about 450 could be obtained from simple interpolations. Once these values were obtained for a few temperatures, a Chebyshev polynomial fit was used to provide κ_2 as a continuous function of temperature. Sample I, with a resistivity ratio of 7.8, required large extrapolations from the data yielding an anomalous temperature dependence for κ_2 . For this reason, another method to evaluate this parameter was explored.

Finnmore¹⁶ has suggested that for "not too pure" samples, κ_2/κ experimentally appears to obey the same temperature dependence (to within about 5%) for a wide range of sample purities. The impurity concentration can be incorporated into¹⁷

$$K = \kappa_2(t=1) = \kappa_0 + 7.53 \times 10^3 \rho_0 \gamma^{1/2},$$

where ρ_0 is the residual resistance in Ω cm, γ is the electronic specific-heat coefficient in $\text{erg}/\text{cm}^3 \text{K}^2$, and κ_0 which equals 0.85 for vanadium,¹⁵

is the intrinsic portion of the Ginzburg-Landau parameter which is independent of the electron mean-free path. The κ_2 temperature dependence for each sample was determined by using a Chebyshev polynomial fit to continuously join the κ_2/κ data of Sekula and Kernohan. The κ value for each sample was determined from Goodman's relation and yielded $\kappa^I = 3.15$, $\kappa^{II} = 0.92$, and $\kappa^{III} = 0.88$. (For reference, κ_2/κ as a function of temperature is shown in Fig. 5.) Comparison of the κ_2 values obtained from this method and the one previously described showed them to agree within 5% for samples II and III, but large discrepancies occurred for sample I.

Because of the extremely low resistivity ratio of sample I, it was felt that neither of the two methods was applicable to this sample. Ostenson and Finnemore¹⁸ have experimentally found that Eilenberger's theory¹⁹ for the temperature dependence of κ_2 agrees rather well with their results when the mean-free path is comparable to the coherence length, but discrepancies arise as sample purity increases.

The results of conductivity measurements (described later in this paper) indicated that the assumption that $l \sim l_0$ was not unreasonable for sample I. It was also assumed that $l = l_{tr}$, the transport mean-free path. Therefore, if $l = (\xi_0 l)^{1/2}$, then $\xi/l_{tr} = (\xi_0 l)^{1/2} \approx 1$. From this information Eilenberger's theory predicts $\kappa = 1.7$, and provides the temperature dependence for κ_2/κ for sample I. This is shown in Fig. 6 which is a reproduction of Fig. 16 in Ref. 21.

(c) *Electron mean-free path l .* The electron mean-free path was determined by fitting the theoretical value of $f(t)$ to the lowest temperature experimental point where the best agreement between theory and experiment is expected. The

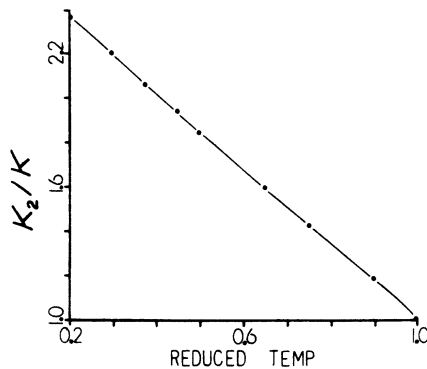


FIG. 5. κ_2 as a function of temperature for samples II and III. Data of Sekula and Kernohan are joined by a polynomial fit to yield κ_2/κ as a continuous function of the reduced temperature.

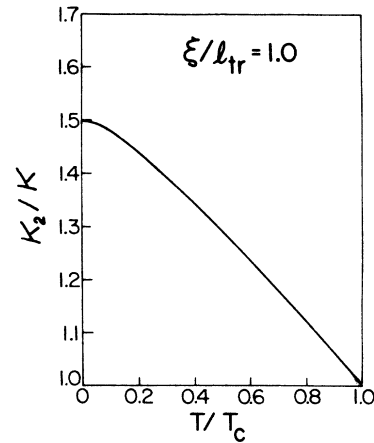


FIG. 6. κ_2/κ as a function of temperature for sample I. Duplication of Fig. 16 in Ref. 21.

function $f(t)$ is completely determined theoretically except for the value of l which could then be extracted from the experimental data. The values thus obtained are $l_I = 5.4 \times 10^{-6}$ cm, $l_{II} = 5.8 \times 10^{-5}$ cm, and $l_{III} = 9.0 \times 10^{-5}$ cm. This mean-free path was found to be independent of temperature and magnetic field for the region of interest in all three samples, indicating an impurity limit l . This determination was based on Pippard's result² that α_n is proportional to l for $ql < 1$. The attenuation in the normal state, arrived at by applying a magnetic field sufficient to turn the sample normal, was found to be independent of temperature from 1.5 °K to T_c . Doubling the applied field also had no effect, indicating that l was independent of the applied field (see Ref. 6).

Up to this point, no mention has been made of the values used for the Fermi velocity and the density of states per spin at the Fermi surface $N(0)$ in the HM expression [Eq. (4)]. The values for the mean-free path indicated above were determined using the phonon enhanced values of $v_F = 1/\langle 1/v \rangle_F$ and $N(0)$ determined by Radebaugh and Keesom.¹⁵ They obtain the density of states per spin from the temperature coefficient of the electronic specific heat

$$\gamma = \frac{2}{3} \pi^2 k_B^2 N(0) = 1.179 \times 10^4 \text{ erg/cm}^3 \text{ K}^2,$$

which is related to the band structure (BS) density of states by $\gamma = \frac{2}{3} \pi^2 k_B^2 (1 + \lambda) N_{BS}(0)$; λ , the phonon enhancement factor, equals one in vanadium.²⁰ This implies that $N(0) = 2N_{BS}(0)$. Also $\langle 1/v \rangle$ over the Fermi surface is

$$\left\langle \frac{1}{v_F} \right\rangle = \frac{\int dS/v}{\int dS} = \hbar \int \frac{dS}{|\nabla_k \epsilon|/S} = \frac{8\pi^3 \hbar N(0)}{S},$$

where $N(0)$ is the phonon-enhanced or band-structure value depending on the desired value for

$\langle 1/v_F \rangle$, and S is the area of the Fermi surface in k -space excluding zone boundaries. Therefore, the phonon-enhanced value of v_F is $\frac{1}{2}$ as large as the band-structure value. The result is that band-structure values for v_F and $N(0)$ yielded mean-free paths twice as large as phonon-enhanced values, i.e., $l_I = 1.1 \times 10^{-5}$ cm, $l_{II} = 1.1 \times 10^{-4}$ cm, and $l_{III} = 1.8 \times 10^{-4}$ cm (band-structure values).

Still another method of arriving at the mean-free path is through the conductivity data taken using a standard four probe dc technique. Based on the relaxation-time approximation to the Boltzmann transport equation,²¹ the dc conductivity may be expressed as

$$\sigma = (e^2/12\pi^2\hbar) l S. \quad (7)$$

Radebaugh and Keesom¹⁵ quote a value of $S/S_F = 0.714$ where S_F represents the area of the Fermi surface for a free-electron gas of density $n = 3.61 \times 10^{23}$ cm⁻³ (they assume five free electrons per atom). Thus, their value for S substituted into Eq. (7) yields values for the mean-free paths of $l_I = 1.3 \times 10^{-6}$ cm, $l_{II} = 4.0 \times 10^{-5}$ cm, and $l_{III} = 6.8 \times 10^{-5}$ cm.

Pippard² has shown that for $ql < 1$, the attenuation due to the electron-phonon interaction should be proportional to $\omega^2\tau$, and for $ql > 1$, proportional to ω . Frequencies high enough to get ql of the order of one were obtainable only in the purest sample. Figure 7 shows a plot of $[\alpha_n(0^\circ\text{K}) - \alpha_s(0^\circ\text{K})]/f$ versus the applied frequency f for sample III, for both longitudinal and transverse waves. Here $\alpha_n(0^\circ\text{K}) - \alpha_s(0^\circ\text{K})$ is a direct measure of the electron-phonon interaction and is therefore the appropriate parameter for this

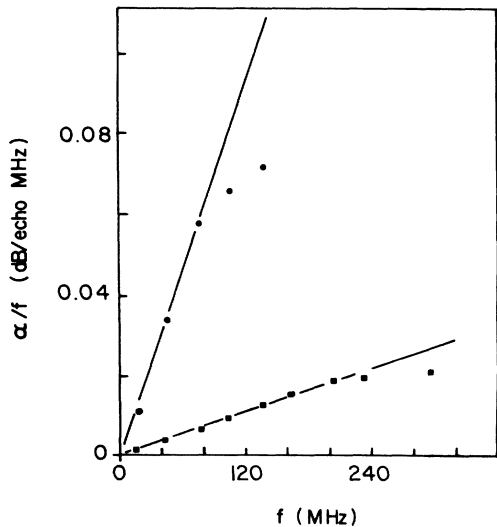


FIG. 7. Attenuation vs frequency in sample III. Data illustrate the onset of the $ql \sim 1$ regime.

plot. The deviation of the experimental points from the extrapolated, small ql , linear dependence of $\Delta\alpha/f$ on f indicates the onset of the $ql \sim 1$ regime. In determining the value of l , the ratio of this deviation to the extrapolated value at a given frequency was compared to the same ratio calculated from Pippard's theory, yielding the value of ql , and thus providing another means of finding the electron mean-free path. (The values obtained from longitudinal and transverse data were found to agree within 20%.) To obtain similar values for l in samples I and II, it was assumed that the low-temperature residual resistance reflected the purity of the sample and therefore the ratio of the residual resistances should be inversely proportional to the ratio of the mean-free paths. The values obtained from this were $l_I = 9.0 \times 10^{-6}$ cm, $l_{II} = 2.9 \times 10^{-4}$ cm, and $l_{III} = 4.1 \times 10^{-4}$ cm.

A different approach might be to use the values of l determined from the Pippard method and, using the conductivity formula [Eq. (7)], solve for S . This method revealed $S/S_F = 0.12$ which is relatively small for a transition metal, but may reflect the fact that the mean-free path (actually the relaxation time) in the conductivity uses a different weighting factor in the integral of the scattering probability over all processes than that used in the ultrasonic attenuation ($ql < 1$).²²

In contrast to this method it might be revealing to insert the Radebaugh and Keesom value of $S = 4.35 \times 10^{17}$ cm⁻² into Pippard's free-electron expression for transverse waves with $ql < 1$;

$$\alpha_t = \frac{1}{5} \frac{Nm v_F}{\rho v_t} q^2 l = \frac{\hbar S^2 f^2}{60\pi^2 \rho v_t^3} l \quad (8)$$

(f is the frequency, v_t is the transverse sound velocity) and solve for l . This method yielded $l_I = 1.61 \times 10^{-6}$ cm, $l_{II} = 6.54 \times 10^{-5}$ cm, and $l_{III} = 1.42 \times 10^{-4}$ cm by using the experimentally found values $\alpha_n^I = 0.0008$ cm⁻¹, $\alpha_n^{II} = 0.03$ cm⁻¹, and $\alpha_n^{III} = 0.09$ cm⁻¹; all at $f = 15$ MHz. Table II lists the

TABLE II. Electronic mean-free paths and methods of determination (all mean-free paths in units of 10^{-6} cm).

Sample	(Γ)	l^a	l^b	l^c	l^d	l^e
I	(7.8)	5.4	11	1.3	9.0	1.6
II	(245)	58	110	40	290	65
III	(450)	90	180	68	410	140

^a Determined from fitting experiment to HM theory using phonon enhanced values for v_F and $N(0)$.

^b Determined from fitting experiment to HM theory using band-structure values for v_F and $N(0)$.

^c Determined from dc conductivity data.

^d Determined from Pippard's relation for $\Delta\alpha/f$ vs f .

^e Determined from Pippard's relation $\alpha_n \sim S^2 l$.

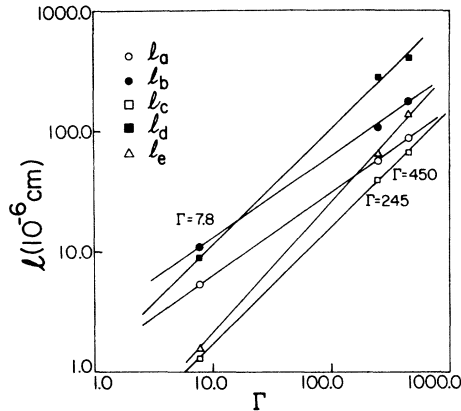


FIG. 8. Relationship between l and Γ as determined from methods listed in Table II.

various values of l and the methods used in determining them. Figure 8 graphically illustrates the relationship found between l and Γ from the various methods.

The slope n of $\ln l_a$ vs $\ln \Gamma$, and therefore power dependence of $l_a \sim \Gamma^n$ is 0.7. Since l_a and l_b only differ by a constant, the slope for l_b is also 0.7. The slope for l_c is 1.0. This is to be expected since Γ is proportional to the conductivity. The slope for l_d is also 1.0; again this follows from the fact that only one of these points was obtained from the frequency dependence of $\Delta\alpha$ and the others were estimated from the ratio of conductivities. The slope for l_e is 1.1 which differs only slightly from the linear relation that is expected. So at least the absolute value of the electron-phonon contribution to the attenuation appears to scale as the conductivity. The principle difference except for proportionality constants appears to be between the slopes of the mean-free paths obtained from the Houghton-Maki theory and the Pippard theory. An arbitrary constant could be understood in terms of using different numbers for some of the parameters since the processes may be taking different averages over the Fermi surface. Perhaps the additional power dependence difference as a function of purity could also be a symptom of this averaging wherein for purer samples the Fermi surface more closely resembles the Fermi surface for pure V.

B. Lower critical field H_{c1}

The primary focus of this research has been on the attenuation near H_{c2} , but some comment should be made on the behavior in the vicinity of H_{c1} .

As the applied magnetic field is increased from zero, there is a point where the flux lines first penetrate the sample. For very pure superconductors, this flux penetration provides additional

scatterers for the thermally excited quasielectrons, thus decreasing their mean-free path.

From BCS theory $\alpha_s/\alpha_n = 2/(e^{\Delta/kT} + 1)$ or $\alpha_s \sim \alpha_n \sim l$, therefore the attenuation should decrease as l decreases [see Fig. 1(b)] until some other mechanism of interaction begins to dominate. This effect has been seen experimentally^{23,24} and theoretically^{24,25} by other researchers.

The sudden rise in the attenuation at H_{c1} for the least pure sample [see Fig. 1(a)] seems reminiscent of the shape of the magnetization curves²⁶ found for vanadium and provides a further indication of the impurity content of this sample. Again, similar behavior has been found in various metallic compounds²⁷ and in a relatively impure sample of niobium²² ($\Gamma = 68$), where the mean-free path is small.

C. Attenuation as a function of temperature, BCS energy gap

It appeared that the two purest samples of vanadium exhibited two energy gaps, a high-temperature gap near T_c , and a low-temperature gap below $t = 0.5$. The apparent discrepancy between the two temperature gaps, approximately 10%, was much less than that obtained by others in niobium,²⁸ but has been seen in vanadium²⁹ before. Because of the temperature limitation of $t \gtrsim 0.3$, the possible deviation in the low-temperature energy gap was too large to provide conclusive results. For this reason the data were visually fitted to the BCS expression $\alpha_s/\alpha_n = 2/(e^{\Delta/kT} + 1)$, with a single energy gap. The results were $2\Delta(0)/kT_c = 3.6 \pm 0.2$, 3.6 ± 0.2 , 2.5 ± 0.2 , with the corresponding critical temperatures reflecting the respective sample impurity concentrations in that $T_c^I = 4.69$ K, $T_c^{II} = 5.26$ K, and $T_c^{III} = 5.27$ K. These critical temperatures compare very favorably with those obtained by extrapolation of the H_{c2} versus temperature data, which were $T_c^I = 4.81$ K, $T_c^{II} = 5.26$ K, and $T_c^{III} = 5.34$ K; the maximum deviation being about 3%. Comparison of these results to those of other researchers²⁹⁻³¹ revealed good agreement within experimental error.

A plot of the BCS theory compared to the digitized experimental points can be seen in Fig. 9.

V. DISCUSSION AND CONCLUSIONS

The Houghton-Maki¹ theory for ultrasonic attenuation in the mixed state predicts that the normalized attenuation can be described in terms of the parameter μ , which, in turn, has been shown to be equal to a well-described function of the temperature times $H_{c2} - H$, i.e., $f(t)\Delta H$, for ΔH small. The experiments performed in three different purity vanadium samples as a function of magnetic field for numerous temperatures very clearly

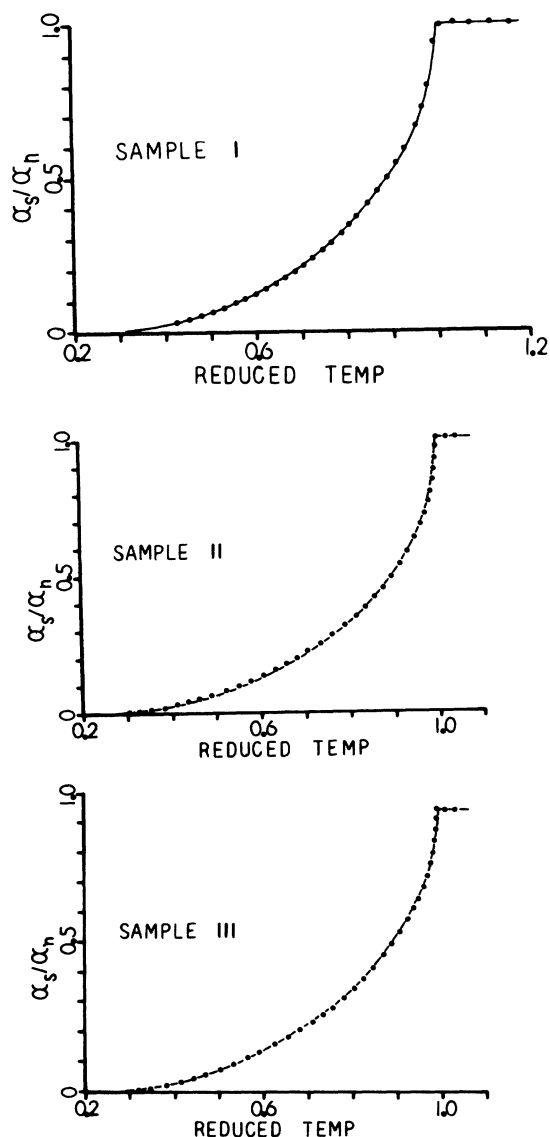


FIG. 9. BCS theory vs experiment in samples I-III. BCS theory vs the digitized experimental points.

manifested the linear dependence of μ on ΔH . The normalized attenuation of a function of μ , as predicted by HM, was found to be in excellent agreement with the experimental results of $\Delta\alpha/\alpha$ vs ΔH , at all temperatures and in all three samples. In sample I, the least-pure sample, the theory agreed with the experimental results through 80% of the mixed state region, $0.8(H_{c2} - H_{c1})$. In samples II and III, the region of comparison was over $0.2(H_{c2} - H_{c1})$, which is much closer to the expected regime of validity since the theory requires that the magnetization be small, and be a linear function of ΔH .

The HM theory also predicts the functional de-

pendence of $f(t)$ on the reduced temperature t . The slopes of the linear plots of μ vs ΔH provided discrete values of $f(t)$; but if the temperature dependence of H_{c2} , κ_2 , and l could be determined, a continuous function, $f(t)$, as prescribed by HM could also be found.

The upper critical field, H_{c2} , was experimentally found to obey the empirical relation

$$H_{c2}(t) = H_{c2}(0) (1 - t^2)/(1 + at^2)$$

with the appropriate values of $H_{c2}(0)$ and a for each sample.

The temperature dependence of κ_2 was not such a universal function for all three samples. The magnetization data of Sekula and Kernohan¹⁴ were used to describe the temperature dependence of κ_2/k for samples II and III, while the κ values were obtained from Goodman's¹⁷ relation $\kappa = \kappa_0 + 7.5 \times 10^3 \rho_0 \gamma^{1/2}$. κ_2 as a function of temperature for sample I (which was considered relatively impure), was determined from the theoretical predictions of Eilenberger¹⁹ for $\xi_0 \approx l$.

The electron mean-free path l was experimentally found to be independent of temperature and magnetic field over the region of interest. For this reason, it was used as a fitting parameter between the discrete and continuous values of $f(t)$ at the lowest temperature, where the theory is expected to be most accurate. The resulting agreement between theory and experiment, illustrated in Fig. 10, was excellent, especially in light of the fact that the HM theory has incorporated the low-temperature limit of $T = 0$ °K in order to arrive at their simple expression for the normalized attenuation in terms of μ .

A comparison of the mean-free paths determined in this manner with those obtained from dc conductivity measurements or from Pippard's predictions for attenuation versus frequency, yields, at most, a factor of 5 in discrepancy. There are several possible explanations for this discrepancy. One, the mean-free path or, what is more readily discussed, the relaxation time, in the conductivity formula [Eq. (7)] uses a different weighting factor in the integral over the scattering probability over all processes that that used in ultrasonic attenuation for $ql < 1$. In dc conductivity, the relaxation time³² is inversely proportional to the weighting factor of $(1 - \cos\theta)$ in favor of large angle scattering; while for $ql \ll 1$, the inverse of the relaxation time for acoustic absorption has a weighting factor²² of $\frac{3}{2}(1 - \cos^2\theta)$. Thus depending on the availability of umklapp processes, the mean-free path as determined from the dc conductivity might be very different from the mean-free path used in the ultrasonic attenuation coefficient. Two, the mean-free path as determined from

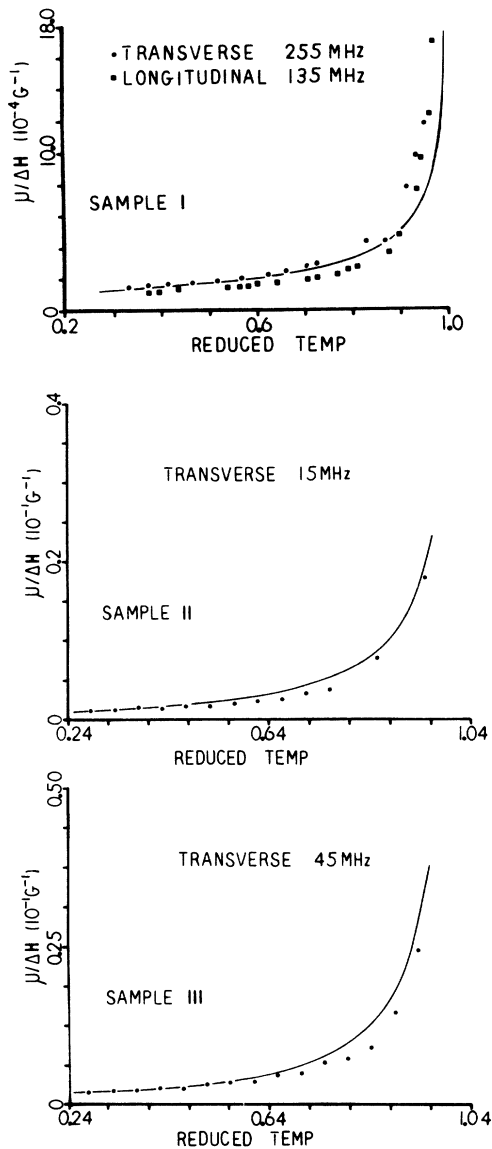


FIG. 10. $\mu/\Delta H$ as a function of reduced temperature for samples I–III. Digitized values vs the continuous values of $f(t)$.

Pippard's free-electron approach neglects real metal^{33–35} effects which have been found to be important even in indium³³ which has a nearly spherical Fermi surface. Bliss and Rayne³³ have shown that the effect of the crystal potential on the Fermi-surface topology is largely responsible for describing the attenuation behavior. They claim that minor modifications to the free-electron Fermi surface, such as the rounding of corners and cusps, are important in determining attenuation values. Their experimental results showed that α/f vs f begins to curve away from the $ql < 1$ extrapolated line before ql is of the order of 1.

Thus, a comparison of the experimental results of this research to the predictions of Pippard's theory could lead to a possible discrepancy of a factor of 2 or 3 in the determination of the acoustic mean-free path of the electrons. Three, the values used for the Fermi velocity and the density of states per spin at the Fermi surface are not well established, at least, as to whether phonon-enhanced or band-structure values should be used. In any case, the HM theory neglects these real metal effects. In light of the possible explanations for disagreement, the final comparison of the discrete values of $f(t)$ determined from the slopes of the μ vs ΔH plots at various temperatures, and the theoretically prescribed, independently determined, continuous values of $f(t)$, illustrates the excellent agreement the HM theory provides in describing ultrasonic attenuation in the mixed state.

There have been other ultrasonic studies of the mixed state in vanadium³⁶ but these have not been as thorough, nor were the results compared to the HM theory. The extensive data presented in this investigation have been shown to be in excellent agreement with the HM theory for $\vec{q} \parallel \vec{H}$ with both longitudinal and transverse waves, and has also indicated the proper dependence on the electronic mean-free path.

Measurements of the ultrasonic attenuation coefficient in the mixed state have also been made on niobium, and the results compared to the HM theory. Carsey and Levy³⁷ found good qualitative agreement for both longitudinal and transverse waves with $\vec{q} \parallel \vec{H}$, but a factor of about 20 was necessary in comparing the HM value with an independently determined value of l . There may be two explanations for this. The first possibility is that, because they did their comparison in the small- μ ($\Delta\alpha/\alpha \sim \mu$) regime, the one-dimensional fluctuation effect, which is dominant in this region, may have contributed to the factor. Another possibility is that the HM theory is valid for low-frequency $ql < 1$ phonons and their frequencies with $0.7 < ql < 3.0$ may have been too high. Purvis *et al.*³⁸ also performed mixed-state ultrasonic measurements on niobium and found a factor of 2 necessary for their agreement, but this factor of 2 arose from comparing the mean-free path from fitting the HM theory to experiment to the conductivity mean-free path. The validity of this comparison has been discussed above. Also, it would appear that a phonon-enhanced value of the density of states was used, but it is not entirely clear whether the band-structure or phonon-enhanced value was used for the Fermi velocity. This may be the reason for the discrepancy.

Purvis *et al.*³⁸ also tested the frequency depen-

dence of the normalized attenuation as a function of magnetic field and found that for any value of ΔH , $\Delta\alpha/\alpha$ monotonically increased as the frequency was increased from 10 to 110 MHz. The opposite frequency dependence was seen by Ikushima *et al.*³⁹ for a frequency range of 25–700 MHz, while no dependence on frequency seen by Forgan and Gough⁴⁰ from 10 to 70 MHz. In each case the experiments were performed on relatively pure ($\Gamma = 1000\text{--}2000$) niobium samples. The HM theory predicts no dependence on frequency for the attenuation coefficient provided $ql < 1$. This prediction has not been thoroughly tested in this work, although transverse waves with $\vec{q} \parallel \vec{H}$ and frequencies of 255 and 135 MHz, propagated in sample I at 1.6, 2.5, and 3.5 K revealed no frequency dependence. It would appear that some definitive experimental work is required to clear up this disagreement.

Another area which has not been thoroughly tested is the HM predictions for acoustic absorption when the phonon wave vector is perpendicular to the applied field. Even at a μ value of 0.2 and $ql < 1$, HM contend that a 30% difference exists between the normalized attenuations of transverse waves with ion motion parallel to, and perpendicular to, the applied field H . Preliminary results on sample I revealed no such difference, although it might be expected that since the electron mean-free path is of approximately the same dimension as the coherence length in this sample, such an anisotropic effect might not be manifested in this relatively impure sample. Therefore, further experiments on the purer samples might reveal interesting results for these orientations, es-

pecially in view of Maki's contention⁴¹ that for $ql > 1$, the attenuation would effectively take different averages of the order parameter simply by rotating the field from $\vec{u} \parallel \vec{H}$ to $\vec{u} \perp \vec{H}$.

It would also appear that the HM theory may have a larger region of validity than they purport. HM contend that the theory should be valid for moderately pure superconductors with the mean-free path much larger than the coherence length, but the results on sample I, where $l \approx \xi_0$, would seem to indicate the theory is applicable over a wider range of purity. To this extent, the experimental results of Tittmann⁴² have been in agreement. Tittmann has performed longitudinal ultrasonic attenuation measurements on a single crystal of V-5.6-at.% Ta with $\xi_0/l \approx 5$. A detailed comparison with the HM theory shows remarkably good agreement indicating that the theory is applicable over a much wider range of purity than expected.

So it seems that the HM theory, as far as it has been tested, provides an accurate description of electron-phonon interaction in the mixed state. Still, there remain areas for further experimental research, and with the production of purer samples the theory may need to incorporate some real metal effects in order to provide a complete description of the mixed state.

The authors would like to thank Dr. Richard Reed of Oak Ridge National Laboratories for providing some of the samples, Dr. Richard Sorbello for many fruitful and enlightening discussions, and Robert Hanson for his help in preparing the samples.

*Research supported by Air Force Office of Scientific Research under AFOSR Grant No. 76-2893.

†Present address: Physics Dept., Wayne State University, Detroit, Mich. 48202.

¹A. B. Pippard, Proc. R. Soc. Lond. **122**, 1104 (1955).

²J. Bardeen, L. N. Cooper, and J. R. Schrieffer, Phys. Rev. **108**, 1175 (1957).

³A. Houghton and K. Maki, Phys. Rev. B **4**, 843 (1971).

⁴K. Maki and T. Tsuzuki, Phys. Rev. **139**, 868 (1965).

⁵U. Brandt, W. Pesch, and L. Tewordt, Z. Phys. **301**, 209 (1967).

⁶J. Waynert, H. Salvo, Jr., and M. Levy, Phys. Rev. **10**, 1859 (1974).

⁷S. Schneider, J. Waynert, M. Levy, and K. Maki (unpublished).

⁸D. J. Thouless, Phys. Rev. Lett. **34**, 946 (1975).

⁹G. Bergman, Z. Phys. **225**, 430 (1969).

¹⁰K. Maki, J. Low-Temp. Phys. **1**, 513 (1969).

¹¹V. L. Ginzburg, Zh. Eksp. Teor. Fiz. **30**, 593 (1955) [Sov. Phys.-JETP **3**, 621 (1956)].

¹²J. A. Osborn, Phys. Rev. **67**, 351 (1945).

¹³J. Auer and H. Ullmaier, Phys. Rev. B **7**, 136 (1973).

¹⁴S. T. Sekula and R. H. Kernohan, Phys. Rev. B **5**, 904 (1972).

¹⁵R. Radebaugh and P. H. Keesom, Phys. Rev. **149**, 217 (1966).

¹⁶D. K. Finnemore (private communication).

¹⁷B. B. Goodman, IBM J. Res. Develop. **147**, 288 (1962).

¹⁸J. E. Ostenson and D. K. Finnemore, APS meeting (March 1975, Denver) (unpublished).

¹⁹G. Eilenberger, Phys. Rev. **153**, 584 (1967).

²⁰R. D. Parker and M. H. Halloran, Phys. Rev. B **9**, 4130 (1974).

²¹See, e.g., J. M. Ziman, *Principles of the Theory of Solids* (Cambridge U. P., Cambridge, 1972).

²²A. B. Bhatia and R. A. Moore, Phys. Rev. **121**, 1075 (1961); M. S. Steinberg, *ibid.* **111**, 425 (1958).

²³A. C. E. Sinclair and J. R. Leibowitz, Phys. Rev. **175**, 596 (1968).

²⁴W. F. Vinen, E. M. Forgan, C. E. Gough, and M. J. Hood, Physica **55**, 94 (1971).

²⁵R. M. Cleary, Phys. Rev. **175**, 587 (1968).

- ²⁶J. J. Wollan, K. W. Haas, J. R. Clem, and D. K. Finne-
more, *Phys. Rev. B* 10, 1874 (1974).
- ²⁷B. R. Tittman, *Phys. Rev. B* 2, 625 (1970).
- ²⁸F. Carsey, R. Kagiwada, and M. Levy, *Phys. Rev. B* 4,
854 (1971).
- ²⁹R. Radebaugh and P. H. Keesom, *Phys. Rev.* 149, 209
(1966).
- ³⁰H. V. Bohm and N. H. Horwitz, *Proceedings of the
Eighth International Conference on Low Temperature
Physics*, edited by R. D. Davies (Butterworths, London,
1963), p. 191.
- ³¹J. L. Brester, M. Levy, and I. Rudnick, *Phys. Rev.*
132, 1062 (1963).
- ³²See, e.g., J. M. Ziman, *Electrons and Phonons* (Ox-
ford U. P., London, 1960).
- ³³E. S. Bliss and J. A. Rayne, *Phys. Rev.* 177, 673
(1969).
- ³⁴L. P. Kadanoff and A. B. Pippard, *Proc. R. Soc. A* 292,
299 (1966).
- ³⁵J. R. Leibowitz, *Phys. Rev.* 136, A22 (1964).
- ³⁶H. Ozaki, K. Kajimura, T. Ishiguro, and N. Mikoshiba,
Phys. Lett. A 28, 300 (1968).
- ³⁷F. Carsey and M. Levy, *Phys. Rev. Lett.* 27, 853
(1971).
- ³⁸M. K. Purvis, R. A. Johnson, and A. R. Hoffman, J.
Phys. Chem. Solids 35, 989 (1974).
- ³⁹A. Ikushima, K. Kajimura, and F. Akao, *Phys. Lett.*
A 25, 151 (1967); K. Kajimura and A. Ikushima, J.
Chem. Phys. Solids 32, 1617 (1971).
- ⁴⁰E. M. Forgan and C. E. Gough, *Phys. Lett. A* 26, 602
(1968).
- ⁴¹K. Maki (private communication).
- ⁴²B. R. Tittman, in *1974 Ultrasonics Symposium Pro-
ceedings*, edited by J. DeKlerk (IEEE, New York,
1974).